Lab on a Chip

PAPER

View Article Online
View Journal | View Issue

Cite this: *Lab Chip*, 2019, **19**, 3979

Microfabricated porous layer open tubular (PLOT) column†

Maxwell Wei-Hao Li, [abc] Jinyan She,[ab] Hongbo Zhu,[ab] Ziqi Li[ad] and Xudong Fan *[ab]

Received 6th September 2019,
Accepted 18th October 2019

DOI: 10.1039/c9lc00886a

rsc.li/loc

Development of micro gas chromatography (μGC) is aimed at rapid and *in situ* analysis of volatile organic compounds (VOCs) for environmental protection, industrial monitoring, and toxicology. However, due to the lack of appropriate microcolumns and associated stationary phases, current μGC is unable to separate highly volatile chemicals such as methane, methanol, and formaldehyde, which are of great interest for their high toxicity and carcinogenicity. This inability has significantly limited μGC field applicability. To address this deficiency, this paper reports the development and characterization of a microfabricated porous layer open tubular (μPLOT) column with a divinylbenzene-based stationary phase. The separation capabilities of the μPLOT column are demonstrated by three distinct analyses of light alkanes, formaldehyde solution, and organic solvents, exhibiting its general utility for a wide range of highly volatile compounds. Further characterization shows the robust performance of the μPLOT column in the presence of high moisture and at high temperatures (up to 300 °C). The small footprint and the ability to separate highly volatile chemicals make the μPLOT column highly suitable for integration into μGC systems, thus significantly broadening μGC's applicability to rapid, field analysis of VOCs.

Gas chromatography (GC) is a powerful tool for separation and analysis of volatile compounds. However, the large size, heavy weight, long analysis time, high power consumption, and high cost of benchtop GC instruments hinder their use in on-site analysis and real-time monitoring. Miniaturized components for micro gas chromatography (μGC) are currently in development to address these issues and enable GC use in field applications.[1–13] Special focus is placed on using microfabrication techniques to miniaturize separation columns, which are the core components of GC systems.[1,3,4,6,10] Monolithic integration of these microcolumns with heaters and other micro-components allows for dead volume minimization and rapid, highly uniform column heating, enabling their use for fast, low-power, and portable μGC technology.[1–3,5,7,9,11,13–16] Current limitations that inhibit the more widespread use of microcolumns include stationary phase pooling in sharp corners (resulting in peak broadening),[1,3,4,6] the lack of fine control over temperature and pressure programming,[1,14,16] and limited variety of stationary phase coatings and techniques (when compared to commercial capillary columns).[17–20] More recently, optimization of fluidic channel layouts, column chip materials, and channel cross-section shapes has improved microcolumn efficiency,[1,3,4,6] while integration with temperature and pressure sensors has allowed for better characterization and control over column temperature and flow rate.[1,3,7,14,16] These advances enable exploration of various microcolumn stationary phases, which in turn has applications for portable and multidimensional μGC.[8,9,11,17–22]

One of the major applications of portable μGC is environmental analysis of highly volatile compounds. EPA Methods 502, 524.2, and 8260 (B, C, D) list a wide range of volatile organic compounds (VOCs) that have varying degrees of toxicity or carcinogenicity; other light volatiles such as formaldehyde and light hydrocarbons are also of interest as common toxic air pollutants.[23–30] Since many common types of columns (*e.g.*, packed, various polysiloxane and polyethylene glycol stationary phases) only weakly retain these light VOCs, porous layer open tubular (PLOT) columns have been developed as an alternative for separating these compounds.[17–19,22,23,31–40] Previous research has highlighted alumina, molecular sieves, carbon sieves, metal–organic frameworks, covalent organic frameworks, and porous

[a] *Department of Biomedical Engineering, University of Michigan, Ann Arbor, MI 48109, USA. E-mail: xsfan@umich.edu*
[b] *Center for Wireless Integrated MicroSensing and Systems (WIMS²), University of Michigan, Ann Arbor, MI 48109, USA*
[c] *Department of Electrical Engineering and Computer Science, University of Michigan, Ann Arbor, MI 48109, USA*
[d] *School of Precision Instruments and Opto-electronics Engineering, Tianjin University, P. R. China*

† Electronic supplementary information (ESI) available. See DOI: 10.1039/c9lc00886a

polymers as PLOT column stationary phase materials.[31,32,34–37] Alumina is known to exhibit high specificity to light hydrocarbon VOCs, while molecular sieve stationary phases are capable of separating fixed gases such as O_2, N_2, and noble gases.[17,19,31,34,36] Divinylbenzene (DVB) polymers do not separate these compounds as strongly, but their excellent stability in the presence of moisture is a highly desirable property for field analysis, where varying ambient conditions can affect μGC separation characteristics.[17,18,31,34,36] Although many capillary based PLOT columns have been researched extensively and are now commercially available, little research has been directed towards the development of microfabricated PLOT columns for portable μGC, which considerably limits μGC's applicability to analysis and monitoring of highly volatile VOCs.

This paper reports the design, fabrication, and evaluation of microfluidic PLOT columns (μPLOT) with a DVB-based stationary phase. The fabrication and column coating procedures are detailed herein, and three benchmarks, *i.e.*, separation of highly volatile alkanes, formaldehyde solution, and organic solvents, are shown to demonstrate the μPLOT column's ability to separate highly volatile VOCs. Characterization of moisture and temperature robustness is also performed. These benchmarks show how the μPLOT column can significantly broaden the applications of μGC in field and environmental analysis of highly volatile VOCs—especially those that are toxic and/or carcinogenic—due to its small footprint, high moisture resilience, and rapid separation capabilities.

Experimental

Materials

All reagents used in this study were purchased from Sigma-Aldrich (St. Louis, MO) and Cal Gas Direct (Huntington Beach, CA). Benchmark reagents: methanol, ethanol, propanol, butanol, dichloromethane, 1,2-dichloroethane, 2-butanone, chloroform, 1,4-dioxane, tetrachloroethylene, formaldehyde solution, methane, ethane, propane, butane, pentane, and hexane. Coating reagents: divinylbenzene, octane, toluene, styrene, azobisisobutyronitrile, acetone, and 3-(trimethoxysilyl)propyl methacrylate. Hysol® 1C™ epoxy was purchased from Ellsworth Adhesive (Germantown, WI). Polyimide sealing resin (P/N 23817) for the connection interface was purchased from Sigma-Aldrich (St. Louis, MO). Deactivated fused silica tubing (P/N 10010) with a 250 μm inner diameter and an Rt-Q-BOND PLOT column (P/N 19765, cut to 5 m in length) were purchased from Restek. N-Type silicon wafers (P/N 1095, 100 mm diameter, 500 μm thickness) and Borofloat 33 glass (P/N 517) were purchased from University Wafer. All materials were used as purchased without further purification or modification.

Microcolumn fabrication

The microcolumn fabrication process is shown in Fig. 1(A). A 3 μm thick layer of thermal oxide was grown on a double side polished silicon wafer and subsequently patterned using standard lithography processes. The exposed oxide was etched away in buffered hydrofluoric acid. The photoresist was then removed, and the wafer was aligned and patterned again to expose the inlets and outlets. A 200 μm deep trench was created *via* deep reactive ion etching. The photoresist was stripped again, and deep reactive ion etching was applied to the entire pattern area. The final column width and depth were both 160 μm, and the width and depth of the inlets and outlets were 400 μm. The final column length was 5 m. The wafer was subsequently anodically bonded with Borofloat 33 glass at 350 °C under vacuum. The heater was deposited on the back side of the column through physical vapor deposition and patterned by lift-off. Photos of the column and heater are provided in Fig. 1(B).

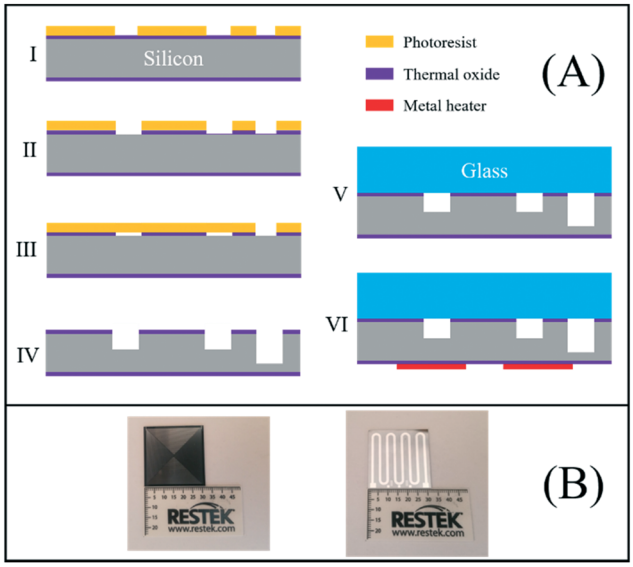

Fig. 1 (A) Microcolumn fabrication processes. I. Soft mask of photoresist exposing both column and inlets/outlets. II. Creation of an oxide hard mask through DRIE. III. Soft mask exposing only inlets/outlets for DRIE etching to 160 μm. IV. DRIE on the entire pattern area to etch inlets/outlets to 400 μm and column to 160 μm. V. Anodic bonding with Pyrex glass to seal the column. VI. Metal heater deposition on the column backside. (B) Photographs of the front (column) and back (heater) sides of the microcolumn. The final column width and depth were both 160 μm. The total column length was 5 m.

Microcolumn coating

The microcolumn was coated based on an optimized procedure adapted from previous research.[32,41] Prior to coating, the column was silanized by eight repeated injections of hexamethyldisilazane vapor under a 0.5 mL min^{-1} flow of helium. Following silanization, the column was washed sequentially with dichloromethane, water, and acetone. Subsequently, the column was filled with a 30 wt% solution of 3-(trimethoxysilyl)propyl methacrylate in acetone—in order to promote adhesion of the coating solution to the column wall—and left to react at room temperature for 15 hours. The column was then washed with acetone and dried using nitrogen.

A polymerization mixture of 32% DVB, 8% styrene, 52% 1-octanol, 8% toluene, and azobisisobutyronitrile (1% w.r.t. DVB) was prepared and heated at 60 °C for 20 hours. The column was filled with the solution, then dry air was used to push the solution out at a rate of 1 cm min^{-1} (approx. 2 psi pressure, see Fig. 2(A)). A dummy column was attached to the end of the column during this process in order to maintain a constant flow resistance. The column was subsequently purged with dry air and crosslinked at 80 °C for 2 hours, followed by post deactivation using hexamethyldisilazane and subsequent baking at 200 °C for 2 hours. The coating process was repeated by filling the column with the same polymerization mixture and pushing the solution out at 1 cm min^{-1}, this time without a dummy column (approx. 2 psi pressure). The second coating step ensured a sufficient coating thickness and enhanced the separation capability of the μPLOT column. The column was crosslinked, deactivated, and baked again (200 °C for 2 hours followed by 300 °C for 2 hours). A photo of the coated column is provided in Fig. 2(B).

Connection interface

Fused silica capillaries with outer diameters of 380 μm and inner diameters of 250 μm were inserted into the inlet and outlet of the μPLOT column. Previously, adhesives such as Hysol® epoxy, polyimide, and Duraseal have been explored to form connection interfaces between capillaries and microcolumn chips. While Hysol® epoxy can withstand the shear force induced by the thermal expansion mismatch between the adhesive and column at 300 °C, strong outgassing prevents operation beyond 200 °C. Polyimide is a thermally stable and outgassing-free material commonly used for outer surface coating of GC columns. However, poor adhesion between polyimide and silicon results in leakage after thermal cycling, which is exacerbated when the microcolumn is under high head pressure. In this work, a two-step gluing method using both polyimide and Hysol® epoxy was developed to form the connection interface (Fig. S1†). Polyimide was first applied to the outer capillary surface, serving as an "O-ring" to prevent the chemicals released by Hysol® epoxy from entering the microcolumn. The capillaries were inserted into microcolumn inlet and outlet and the chip was heated at 120 °C overnight to further cure the polyimide. Hysol® epoxy was subsequently applied to the outer surface of the connection interface and cured at 120 °C for four hours. The connection was tested using a helium leak detector after 15 cycles up to 300 °C (ramping from 120 °C to 300 °C at 30 °C per min) and showed no signs of leakage or damage.

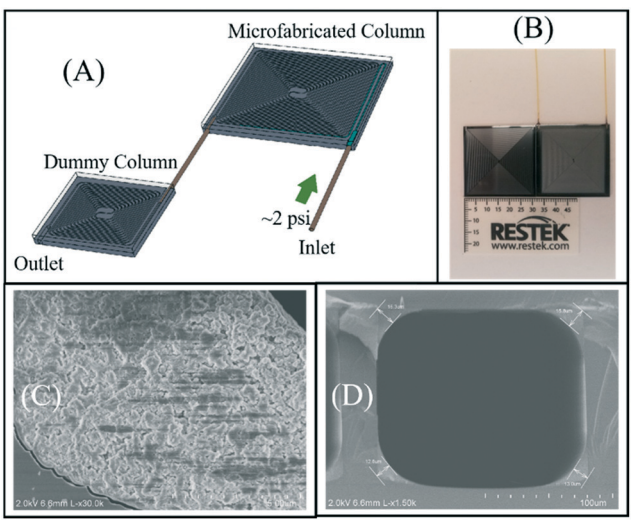

Fig. 2 (A) Microcolumn coating setup. The column was statically coated by filling with the polymerization mixture and subsequently pushing the mixture out with a pressure of 2 psi. The microcolumn was coated a second time using the same 2 psi pressure and the same polymerization mixture without the dummy column. (B) Photograph of the μPLOT column (right) with an uncoated microcolumn (left) for comparison. (C) SEM image of μPLOT porous polymer coating inside the silicon channel. (D) Image of film coating on the channel cross section, with stationary phase pooling observed at column corners. The thickest porous layer at the corner ranges from about 13–16 μm. The average thickness of the porous layer along the border is about 1.83 μm. A zoom in of the column wall is provided in Fig. S2.† A zoom-in of the column surface is provided in Fig. S3.†

Experimental setup

The μPLOT column was evaluated on all separations using an Agilent 6890 benchtop GC equipped with an injection port and a flame ionization detector (FID). Temperature ramping was controlled by the GC oven. Ultra-high purity 5.0 grade helium was used as the carrier gas.

Results and discussion

Stationary phase characterization

To characterize the polymer stationary phase, the μPLOT column was frozen in liquid nitrogen and cut open. The stationary phase was imaged by scanning electron microscopy (SEM), which allowed for observation of the polymer's porous nature (Fig. 2(C) and (D)). It is found that the stationary phase tends to pool around the corners of the microcolumn, which does not occur for regular capillary columns. The average film thickness along the column wall is estimated by approximately calculating the area of the stationary phase pooled at the corners (using triangular approximations) and dividing by the total cross-section border length (~630 μm). This yielded an average film thickness of 1.83 μm. Experimentation with the coating thickness showed that the second coating step described in the "Microcolumn coating" section is important to ensure a porous layer with sufficient thickness. Inferior separation performance was observed with μPLOT columns with a single coating step.

Separation of highly volatile alkanes

The ability to separate light hydrocarbons is essential for GC columns and has applications in analysis for the petroleum

industry, feedstock products, and environmental monitoring.[11,23,34,35,37,38] This benchmark presents analysis of highly volatile alkanes, C_1 to C_6. The temperature was ramped from 40 °C to 160 °C at 30 °C per min at a carrier gas flow rate of 3 mL min^{-1} (measured at 40 °C). The resulting chromatogram is presented in Fig. 3. All six alkanes are clearly separated by the μPLOT column, with retention times and full widths at half maxima (FWHMs) reported in Table 1. Tailing factors are also provided and are used for discussion in the Separation of organic solvents and moisture robustness section.

Formaldehyde separation

Formaldehyde is a colorless, odorous gas widely used in building materials and household products, and also serves as a preservative for tissue fixation. A causal relationship between exposure to formaldehyde and cancer in humans has been determined by various epidemiological studies, leading to increasing concern over industrial and environmental monitoring of airborne exposure.[24–30,42] Previous research has shown that sensitive formaldehyde detection is possible *via* portable GC separation using a Restek Q-BOND PLOT column.[43] The following benchmark (Fig. 4) demonstrates the μPLOT column's ability to replicate this separation, suggesting that the μPLOT column may be used as an alternative to commercial capillary columns for portable μGC devices. A mixture of formaldehyde solution (containing, additionally, water and methanol), ethanol, and 1-propanol was used for injection. The temperature was ramped from 120 °C to 180 °C at 30 °C per min with a carrier gas flow rate of 1.1 mL min^{-1} (measured at 120 °C). Note that the formaldehyde peak is relatively small and the water peak is absent due to the FID's poor sensitivity to these chemicals.

Fig. 4 shows that formaldehyde is fully separated from methanol, ethanol, and 1-propanol with a retention time of 1.389 min and a peak FWHM of 0.073 min. Resolutions between adjacent peaks (defined by eqn (1)) are provided in Table 2.

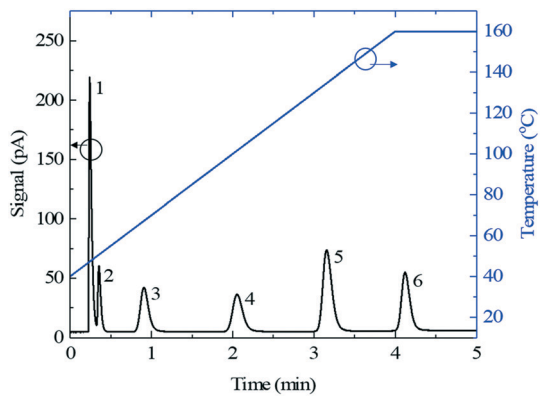

Fig. 3 Separation of light alkanes. A splitless injection of 10 μL of headspace vapor from a mixture of 6 alkanes was made. Carrier gas flow rate: 3 mL min^{-1} at 40 °C. 1. Methane; 2. ethane; 3. propane; 4. butane; 5. pentane; 6. hexane. Analysis is provided in Table 1.

Table 1 Analysis of μPLOT separation of C_1 to C_6 alkanes. Not all tailing factors could be directly calculated using eqn (2); these are marked with a * and are calculated by using the lowest possible peak height instead (ethane[(2)]: 9%)

	Retention time (min)	FWHM (min)	Tailing factor
Methane[(1)]	0.2416	0.0337	2.5372
Ethane[(2)]	0.3551	0.0385	1.3229*
Propane[(3)]	0.9083	0.1088	1.2687
Butane[(4)]	2.0521	0.1370	1.2694
Pentane[(5)]	3.1556	0.1245	1.3325
Hexane[(6)]	4.1236	0.1140	1.2838

$$R = 1.18 \times \frac{t_2 - t_1}{w_1 + w_2}, \quad (1)$$

where t_1 and t_2 are the retention times of the first and second peaks, respectively. w_1 and w_2 are the FWHMs of the first and second peaks, respectively.

Since pure formaldehyde is highly reactive, stress testing of the μPLOT column was performed by repeated injections of formaldehyde vapor to assess potential column degradation. The formaldehyde solution was heated to 80 °C to increase the sample volatility prior to injection. 200 μL vapor samples were drawn from the headspace and injected 30 times using the same temperature profile and flow rate as above. The formaldehyde solution was then allowed to cool, and separation of methanol, ethanol, 1-propanol, and formaldehyde was performed again post-stress testing. Analysis of retention times, FWHMs, and resolutions shows that injection of formaldehyde vapor caused no significant degradation of the column stationary phase (see Table 2, *p*-values between pre- and post-stress testing are all above 0.6, with a significance level of $p = 0.05$).

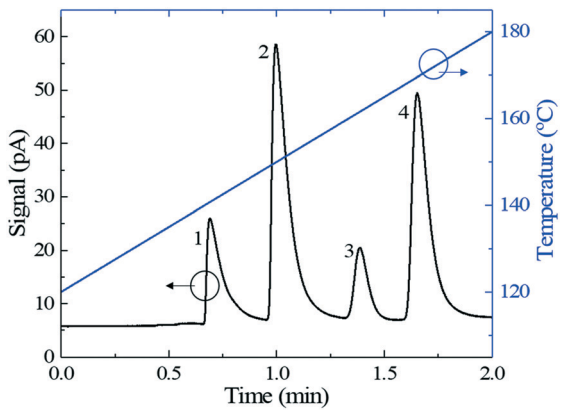

Fig. 4 Separation of formaldehyde from methanol, ethanol, and 1-proponal. 200 μL of headspace vapor from a formaldehyde solution (37 wt% in water with 10–15% of methanol as a stabilizer) was mixed with 50 μL of headspace vapor from a mixture of ethanol and 1-propanol. A splitless injection was made into the injection port of an Agilent 6890 benchtop GC. Carrier gas flow rate: 1.1 mL min^{-1} at 120 °C. 1. Methanol; 2. ethanol; 3. formaldehyde; and 4. 1-propanol. Analysis is provided in Table 2.

Table 2 Analysis of μPLOT separation of methanol(1), ethanol(2), formaldehyde(3), and 1-propanol(4) pre- and post-stress testing. Retention times (RT), FWHMs, and resolutions are provided as averages over 5 runs along with corresponding standard deviations. *p*-Values are calculated between pre- and post-stress testing values, with significance taken at $p = 0.05$. All *p*-values are greater than 0.6, showing no significant difference after stress testing with formaldehyde vapor

	Pre-stress test	Post-stress test	*p*-Value
Methanol(1) RT	0.6748 ± 0.014	0.6735 ± 0.009	0.916
Methanol(1) FWHM	0.0752 ± 0.005	0.0747 ± 0.001	0.867
Ethanol(2) RT	0.9657 ± 0.022	0.9583 ± 0.017	0.709
Ethanol(2) FWHM	0.0783 ± 0.004	0.0796 ± 0.004	0.712
Formaldehyde(3) RT	1.3552 ± 0.025	1.3476 ± 0.018	0.726
Formaldehyde(3) FWHM	0.0773 ± 0.005	0.0785 ± 0.004	0.791
1-Propanol(4) RT	1.6100 ± 0.033	1.6101 ± 0.018	0.995
1-Propanol(4) FWHM	0.0878 ± 0.005	0.0884 ± 0.004	0.863
Resolution (1, 2)	2.2472 ± 0.186	2.1820 ± 0.126	0.672
Resolution (2, 3)	2.9636 ± 0.173	2.9134 ± 0.155	0.744
Resolution (3, 4)	1.8288 ± 0.166	1.8598 ± 0.097	0.784

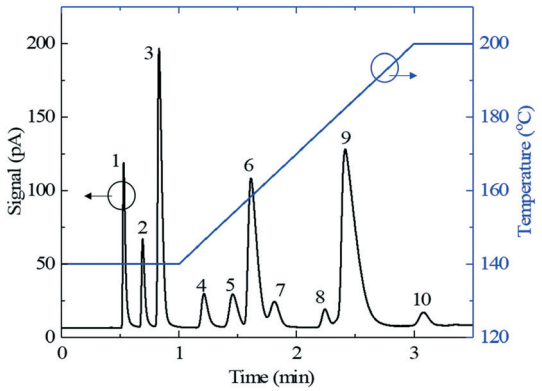

Fig. 5 Separation of organic solvents. A splitless injection of 100 μL of headspace vapor from a mixture of 10 solvents was made. Carrier gas flow rate: 1.1 mL min^{-1} at 140 °C. 1. Methanol; 2. ethanol; 3. dichloromethane; 4. 2-butanone; 5. 1-propanol; 6. 1,2-dichloroethane; 7. chloroform; 8. 1-butanol; 9. 1,4-dioxane; 10. tetrachloroethylene. Analysis is provided in Table 3.

Separation of organic solvents and moisture robustness

The purpose of this benchmark is two-fold. First, organic solvents are used in a wide variety of industries (*e.g.*, pharmaceuticals, manufacturing, and agriculture), many of which are listed as toxic or carcinogenic. Real time monitoring of these compounds by portable μGC would be facilitated by efficient separation using the μPLOT column. Second, the stability and performance of separation columns —especially those for field applications—in the presence of moisture are of concern for samples containing water or solvents. Since moisture can affect retention times and result in peak tailing and broadening, a hydrophobic stationary phase (*i.e.*, DVB) can reduce the severity of these effects. In this benchmark, a sample of ten solvents (Table 3) was separated using the μPLOT column, as shown in Fig. 5. The temperature was ramped from 140 °C to 200 °C at 30 °C per min with a carrier gas flow rate of 1.1 mL min^{-1} (measured at 140 °C). Retention times and peak FWHMs are provided in Table 3.

Table 3 Retention times, FWHMs, and tailing factors of organic solvents separated by the μPLOT column. Not all tailing factors could be directly calculated using eqn (2); these are marked with a * and are calculated by using the lowest possible peak height instead (1-propanol(5): 11%, chloroform(7): 42%, 1-butanol(8): 27%)

	Retention time (min)	FWHM (min)	Tailing factor
Methanol(1)	0.5291	0.0222	1.9737
Ethanol(2)	0.6907	0.0282	1.7977
Dichloromethane(3)	0.8301	0.0388	1.8842
2-Butanone(4)	1.2122	0.0605	1.4656
1-Propanol(5)	1.4587	0.0785	1.2607*
1,2-Dichloroethane(6)	1.6109	0.0827	1.8831
Chloroform(7)	1.8119	0.0908	1.0093*
1-Butanol(8)	2.2416	0.0618	1.1705*
1,4-Dioxane(9)	2.4166	0.1317	2.1957
Tetrachloroethylene(10)	3.0791	0.0922	1.1676

Robustness against moisture was assessed by examining peak shapes. Table 3 also reports the tailing factor (defined in eqn (2)) for each peak.

$$\mathrm{TF} = \frac{p_t - p_f}{2(p_m - p_f)}, \quad (2)$$

where p_f is the time of the peak front (measured at 5% of the peak height), p_t is the time of the peak tail (also measured at 5% of the peak height), and p_m is the time of the peak maximum (*i.e.* the retention time).

A tailing factor of 1 represents a perfectly symmetric peak, but is not expected from the μPLOT column due to stationary phase pooling in sharp microcolumn corners. The tailing factors in Table 3 are instead compared to tailing factors calculated from the alkane separation (Table 1), a gaseous sample containing no moisture. While, on average, tailing factors for the solvent separation are higher than those for the alkane separation, peaks of similar heights (*e.g.*, methane and methanol/dichloromethane, butane and 2-butanone/tetrachloroethylene) show comparable tailing factors. This suggests that the effects of peak broadening and tailing in the solvent separation, if due to moisture, are relatively minor and may be by-products of other factors such as separation parameters (temperature, flow rate), sampling injection amount, and varying retention times for polar and nonpolar compounds.

Further assessment of the μPLOT column's stability in the presence of moisture was examined by adding water to injected samples. 100 μL of headspace vapor from a formaldehyde solution (diluted to 20 wt% in methanol) was injected, along with 0, 100, 200, 300, and 400 μL of water vapor. The water was heated to 80 °C in order to increase the partial pressure in the headspace. The temperature was ramped from 90 °C to 150 °C at 30 °C per min with a carrier gas flow rate of 2 mL min^{-1} (measured at 90 °C). Sample chromatograms are provided in Fig. 6(A) and (B) (injections with 0 and 400 μL of

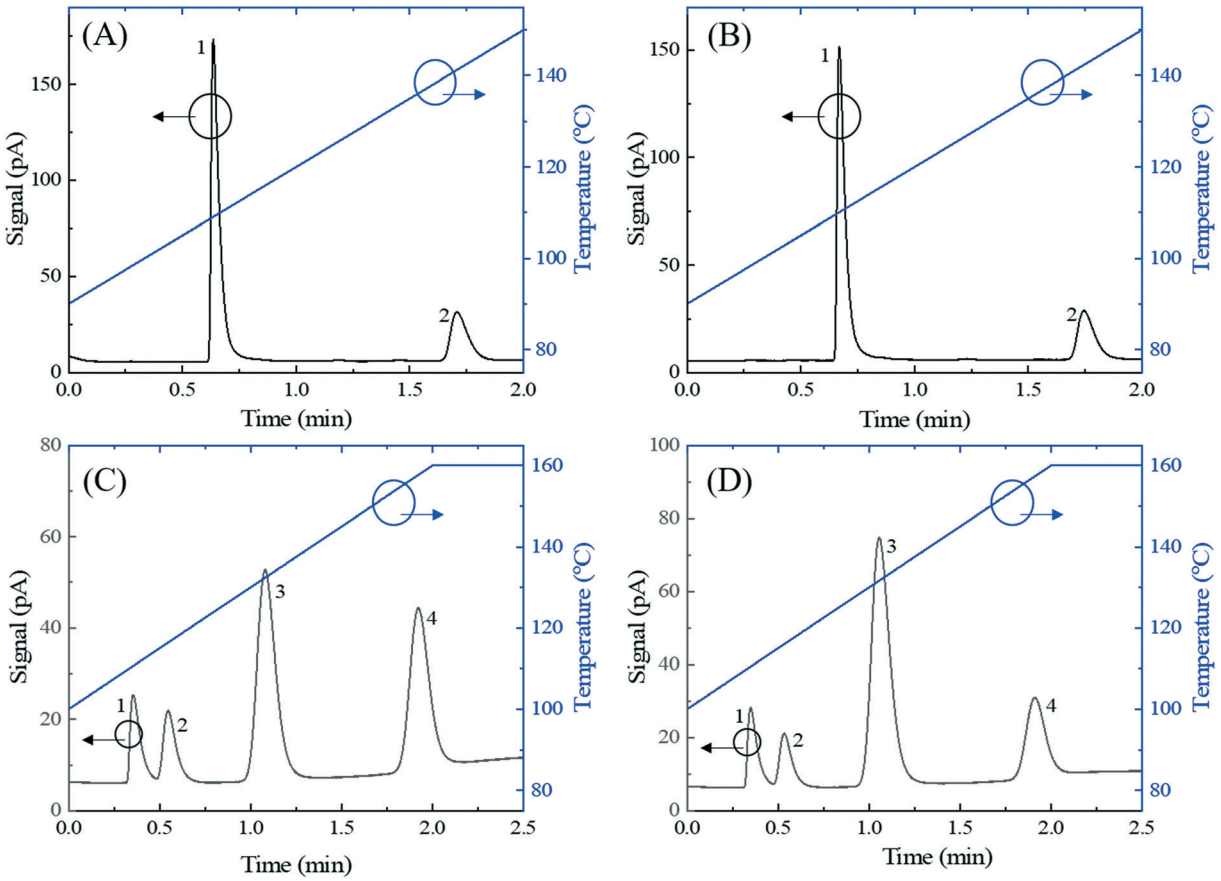

Fig. 6 Separation of methanol[(1)] and formaldehyde[(2)] with no added moisture (A) and with 400 μL of additional water vapor (B). 100 μL methanol and formaldehyde vapor was obtained from the headspace of the previously used formaldehyde solution diluted to 20 wt% in methanol. Carrier gas flow rate: 2 mL min^{-1} at 90 °C. Separation of propane[(1)], butane[(2)], pentane[(3)], and hexane[(4)] with no added moisture (C) and with 500 μL of additional water vapor (D). A splitless injection of 5 μL of headspace vapor from a mixture of the alkanes was made. Carrier gas flow rate: 1.3 mL min^{-1} at 100 °C.

water vapor). Retention times, peak widths, and tailing factors are analyzed as shown in Fig. 7. *p*-Values between injections with 0 and 400 μL of water vapor are provided in Table 4(A) (significance taken at $p = 0.05$). Notably, all retention times and FWHMs show no significant difference when moisture is added to the sample, demonstrating the μPLOT column's moisture resistance. Alkanes C_3 to C_6 were also injected with 0 and 500 μL of water vapor (heated to 80 °C) with a temperature ramping profile of 100 °C to 160 °C at 30 °C per min with a carrier gas flow rate of 1.3 mL min^{-1} (measured at 100 °C). Sample chromatograms are shown in Fig. 6(C) and (D) and analysis is provided in Table 4(B). Again, no significant differences in retention times or FWHMs were observed. Additional information is provided in Fig. S4 and S5, and Tables S1 and S2.†

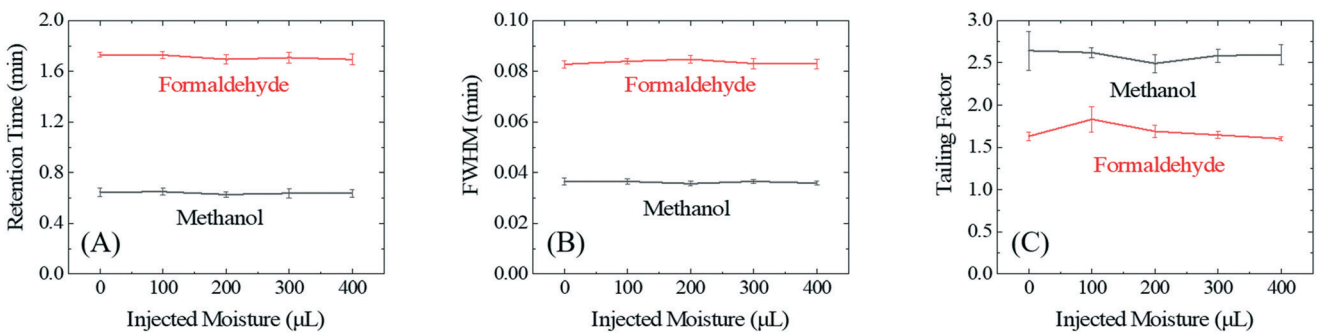

Fig. 7 Methanol and formaldehyde retention times (A), FWHMs (B), and tailing factors (C) with 0 and 400 μL of injected moisture. Error bars represent one standard deviation and are calculated from 5 repetitions.

Table 4 (A) *p*-Values between retention times (RTs) and FWHMs of methanol and formaldehyde with no added moisture and 400 μL of added moisture (5 runs each). (B) *p*-Values between RTs and FWHMs for C_3 to C_6 with no added moisture and 500 μL of added moisture (5 runs each). Significance was taken at $p = 0.05$; all *p*-Values are over 0.4, showing no significant difference in performance with added moisture

(A)	*p*-Value
Methanol[(1)] RT	0.573
Methanol[(1)] FWHM	0.526
Formaldehyde[(2)] RT	0.554
Formaldehyde[(2)] FWHM	0.904
(B)	
Propane[(1)] RT	0.740
Propane[(1)] FWHM	0.419
Butane[(2)] RT	0.751
Butane[(2)] FWHM	0.947
Pentane[(3)] RT	0.732
Pentane[(3)] FWHM	0.704
Hexane[(4)] RT	0.710
Hexane[(4)] FWHM	0.457

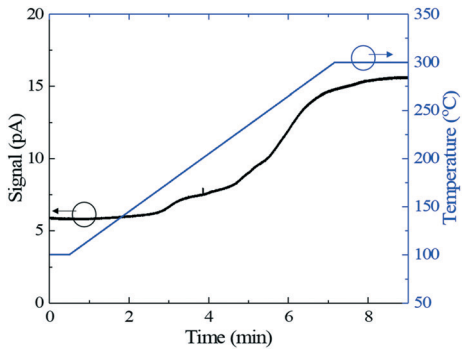

Fig. 8 μPLOT bleed profile with the temperature ramping to 300 °C.

The column's performance under high temperature was also analyzed by temperature ramping from 100 °C (held for 0.5 min) to 300 °C at 30 °C per minute with a carrier gas flow rate of 2 mL min^{-1} (measured at 100 °C). The bleed profile is provided in Fig. 8. The average baseline signal ranged from 5.845 pA (measured from 0.01 to 0.5 min) to 15.374 pA (measured from 8 to 8.5 min). The relatively low stationary phase bleeding at 300 °C suggests that the μPLOT column can be operated at high temperatures for separation of heavier compounds. However, it should be noted that operation at 300 °C with the μPLOT column should be limited to a short amount of time. After heating the column to 250 °C for 3 hours, some degradation in performance was observed (only 9 of the solvents could be separated, with 1,2-dichloroethane and chloroform being coeluted with the same experimental parameters as in Fig. 5). However, the column is robust at 210 °C, capable of sustaining over 14 h of operation at this temperature without noticeable degradation.

Finally, the μPLOT column's separation performance was compared with a commercial Restek Q-BOND PLOT column (see Fig. S6 and Table S3†) by measuring each column's height equivalent to the theoretical plate (HETP) with methanol and butane. The μPLOT column's HETPs for methanol and butane were 1.156 and 0.974 mm, respectively, compared to the Q-BOND PLOT column's 0.697 and 0.617 mm. The μPLOT column's HETP is up to 66% higher than the Q-BOND PLOT column's, which is likely due to stationary phase pooling (see the Stationary phase characterization section) resulting in broader peaks and greater peak tailing. Another possible cause could be particles trapped within the column channel, which trap analytes and further increase broadening. A lower HETP can be achieved by coating the column multiple times (*i.e.*, more than twice).

Conclusion

The microfabrication and coating of a chip-based PLOT column has been described herein. This μPLOT column demonstrated separation of light alkanes, formaldehyde solution, and organic solvents as well as robustness to moisture and temperatures of at least 210 °C. Combined with the μPLOT column's small footprint, the ability to efficiently separate a wide range of highly volatile compounds makes the μPLOT column highly suitable for use in portable GC field analysis. In particular, the μPLOT column can broaden μGC's applicability to on-site monitoring of toxic and carcinogenic compounds, many of which are light VOCs that are difficult to separate with other common stationary phases in existing microcolumns (*e.g.*, polysiloxane or polyethylene glycol based). By enabling a method for real-time analysis of these VOCs, online environmental and pollution control also becomes possible. More specialized, selective separations (*i.e.*, more suitable to specific groups of chemicals) can be obtained by tuning the stationary phase composition, while higher separation performance can be achieved with a larger number of coatings or by increasing the column length (at the cost of increased separation time and power consumption for portable systems). Further improvements may target peak tailing and broadening due to stationary phase pooling, which can be addressed with additional microfabrication steps to etch column channels with more rounded corners.

Conflicts of interest

There are no conflicts to declare.

Acknowledgements

The authors acknowledge the support from NIOSH under grant R01 OH011082-01A1 and microfabrication aid from the Lurie Nanofabrication Facility at the University of Michigan.

References

1 M. Agah, G. R. Lambertus, R. Sacks and K. Wise, High-speed MEMS-based gas chromatography, *J. Microelectromech. Syst.*, 2006, **15**, 1371–1378.

2 F. Haghighi, Z. Talebpour and A. Sanati-Nezhad, Through the years with on-a-chip gas chromatography: a review, *Lab Chip*, 2015, **15**, 2559–2575.
3 B. P. Regmi and M. Agah, Micro Gas Chromatography: An Overview of Critical Components and Their Integration, *Anal. Chem.*, 2018, **90**, 13133–13150.
4 M. A. Zareian-Jahromi, M. Ashraf-Khorassani, L. T. Taylor and M. Agah, Design, Modeling, and Fabrication of MEMS-Based Multicapillary Gas Chromatographic Columns, *J. Microelectromech. Syst.*, 2009, **18**, 28–37.
5 M. Akbar, M. Restaino and M. Agah, Chip-scale gas chromatography: From injection through detection, *Microsyst. Nanoeng.*, 2015, **1**, 15039.
6 G. Lambertus, A. Elstro, K. Sensenig, J. Potkay, M. Agah, S. Scheuering, K. Wise, F. Dorman and R. Sacks, Design, fabrication, and evaluation of microfabricated columns for gas chromatography, *Anal. Chem.*, 2004, **76**, 2629–2637.
7 G. R. Lambertus, C. S. Fix, S. M. Reidy, R. A. Miller, D. Wheeler, E. Nazarov and R. Sacks, Silicon microfabricated column with microfabricated differential mobility spectrometer for GC analysis of volatile organic compounds, *Anal. Chem.*, 2005, **77**, 7563–7571.
8 W. R. Collin, G. Serrano, L. K. Wright, H. Chang, N. Nunovero and E. T. Zellers, Microfabricated gas chromatograph for rapid, trace-level determinations of gas-phase explosive marker compounds, *Anal. Chem.*, 2014, **86**, 655–663.
9 S. K. Kim, H. Chang and E. T. Zellers, Microfabricated gas chromatograph for the selective determination of trichloroethylene vapor at sub-parts-per-billion concentrations in complex mixtures, *Anal. Chem.*, 2011, **83**, 7198–7206.
10 S. Reidy, G. Lambertus, J. Reece and R. Sacks, High-performance, static-coated silicon microfabricated columns for gas chromatography, *Anal. Chem.*, 2006, **78**, 2623–2630.
11 J. Luong, R. Gras, R. A. Shellie and H. J. Cortes, Applications of planar microfluidic devices and gas chromatography for complex problem solving, *J. Sep. Sci.*, 2013, **36**, 182–191.
12 S. Ali, M. Ashraf-Khorassani, L. T. Taylor and M. Agah, MEMS-based semi-packed gas chromatography columns, *Sens. Actuators, B*, 2009, **141**, 309–315.
13 A. C. Lewis, J. F. Hamilton, C. N. Rhodes, J. Halliday, K. D. Bartle, P. Homewood, R. J. Grenfell, B. Goody, A. M. Harling, P. Brewer, G. Vargha and M. J. Milton, Microfabricated planar glass gas chromatography with photoionization detection, *J. Chromatogr. A*, 2010, **1217**, 768–774.
14 M. Agah, J. A. Potkay, G. Lambertus, R. Sacks and K. D. Wise, High-performance temperature-programmed microfabricated gas chromatography columns, *J. Microelectromech. Syst.*, 2005, **14**, 1039–1050.
15 S. Narayanan and M. Agah, Fabrication and Characterization of a Suspended TCD Integrated With a Gas Separation Column, *J. Microelectromech. Syst.*, 2013, **22**, 1166–1173.
16 S. Reidy, D. George, M. Agah and R. Sacks, Temperature-programmed GC using silicon microfabricated columns with integrated heaters and temperature sensors, *Anal. Chem.*, 2007, **79**, 2911–2917.
17 Restek's PLOT Column Family - The Benchmark for Performance, https://www.restek.com/Technical-Resources/Technical-Library/Petroleum-Petrochemical/Restek-s-PLOT-Column-Family-PCSS1163G-UNV.
18 Z. Ji and S. Hutt, A new bonded porous polymer PLOT U column with increased polarity, *J. Chromatogr. Sci.*, 2000, **38**, 496–502.
19 A. K. Vickers, *PLOT Column Selection*, 2000.
20 V. N. Sidel'nikov, O. A. Nikolaeva and I. A. Platonov, Stationary phases deposition on the planar columns capillaries, *Prot. Met. Phys. Chem. Surf.*, 2015, **51**, 1065–1075.
21 J. R. Hopkins, A. C. Lewis and K. A. Read, A two-column method for long-term monitoring of non-methane hydrocarbons (NMHCs) and oxygenated volatile organic compounds (o-VOCs), *J. Environ. Monit.*, 2003, **5**, 8–13.
22 C. Yu, F. Svec and J. M. J. Fréchet, Towards stationary phases for chromatography on a microchip: Molded porous polymer monoliths prepared in capillaries by photoinitiated in situ polymerization as separation media for electrochromatography, *Electrophoresis*, 2000, **21**, 120–127.
23 N. Pelz, N. M. Dempster and P. R. Shore, Analysis of Low Molecular Weight Hydrocarbons Including 1,3-Butadiene in Engine Exhaust Gases Using an Aluminum Oxide Porous-Layer Open-Tubular Fused-Silica Column, *J. Chromatogr. Sci.*, 1990, **28**, 230–235.
24 W. D. Kerns, K. L. Pavkov, D. J. Donofrio, E. J. Gralla and J. A. Swenberg, Carcinogenicity of Formaldehyde in Rats and Mice after Long-Term Inhalation Exposure, *Cancer Res.*, 1983, **43**, 4382–4392.
25 T. Dumas, Determination of Formaldehyde in Air by Gas-Chromatography, *J. Chromatogr.*, 1982, **247**, 289–295.
26 S. Harrison, Determination of Small Amounts of Formaldehyde in Acetaldehyde, *Analyst*, 1967, **92**, 773–778.
27 X. Tang, Y. Bai, A. Duong, M. T. Smith, L. Li and L. Zhang, Formaldehyde in China: production, consumption, exposure levels, and health effects, *Environ. Int.*, 2009, **35**, 1210–1224.
28 T. Salthammer, S. Mentese and R. Marutzky, Formaldehyde in the indoor environment, *Chem. Rev.*, 2010, **110**, 2536–2572.
29 J. A. Swenberg, W. D. Kerns, R. I. Mitchell, E. J. Gralla and K. L. Pavkov, Induction of Squamous Cell Carcinomas of the Rat Nasal Cavity by Inhalation Exposure to Formaldehyde Vapor, *Cancer Res.*, 1980, **40**, 3398–3402.
30 A. Songur, O. A. Ozen and M. Sarsilmaz, The toxic effects of formaldehyde on the nervous system, *Rev. Environ. Contam. Toxicol.*, 2010, **203**, 105–118.
31 J. de Zeeuw, R. C. M. de Nijs and L. T. Henrich, Adsorption Chromatography on PLOT (Porous-Layer Open-Tubular) Columns: A New Look at the Future of Capillary GC, *J. Chromatogr. Sci.*, 1987, **25**, 71–83.
32 D. Sýkora, E. C. Peters, F. Svec and J. M. J. Fréchet, "Molded" porous polymer monoliths: A novel format for capillary gas chromatography stationary phases, *Macromol. Mater. Eng.*, 2000, **275**, 42–47.

33 E. P. Nesterenko, M. Burke, C. de Bosset, P. Pessutto, C. Malafosse and D. A. Collins, Monolithic porous layer open tubular (monoPLOT) capillary columns for gas chromatography, *RSC Adv.*, 2015, **5**, 7890–7896.

34 Z. H. Ji, R. E. Majors and E. J. Guthrie, Porous layer open-tubular capillary columns: preparations, applications and future directions, *J. Chromatogr. A*, 1999, **842**, 115–142.

35 Y. V. Patrushev and V. N. Sidelnikov, Selection of the porous layer open tubular columns for separation of light components in comprehensive two-dimensional gas chromatography, *J. Chromatogr. A*, 2018, **1579**, 83–88.

36 J. Zhang, J. Chen, S. Peng, S. Peng, Z. Zhang, Y. Tong, P. W. Miller and X. P. Yan, Emerging porous materials in confined spaces: from chromatographic applications to flow chemistry, *Chem. Soc. Rev.*, 2019, **48**, 2566–2595.

37 S. M. Mugo, L. Huybregts and J. Mazurok, Adjustable Methacrylate Porous Monolith Polymer Layer Open Tubular Silica Capillary Microextraction for the Determination of Polycyclic Aromatic Hydrocarbons, *Anal. Lett.*, 2016, **49**, 1824–1834.

38 R. Gras, Y. Hua and J. Luong, High-throughput gas chromatography for volatile compounds analysis by fast temperature programming and adsorption chromatography, *J. Sep. Sci.*, 2017, **40**, 1979–1984.

39 T. J. Causon, R. A. Shellie, E. F. Hilder, G. Desmet and S. Eeltink, Kinetic optimisation of open-tubular liquid-chromatography capillaries coated with thick porous layers for increased loadability, *J. Chromatogr. A*, 2011, **1218**, 8388–8393.

40 M. Blumer, Preparation of porous layer open tubular columns by dynamic coating and rapid conditioning, *Anal. Chem.*, 2002, **45**, 980–982.

41 F. Svec and A. A. Kurganov, Less common applications of monoliths. III. Gas chromatography, *J. Chromatogr. A*, 2008, **1184**, 281–295.

42 B. Daoud Agha Dit Daoudy, M. A. Al-Khayat, F. Karabet and M. A. Al-Mardini, A Robust Static Headspace GC-FID Method to Detect and Quantify Formaldehyde Impurity in Pharmaceutical Excipients, *J. Anal. Methods Chem.*, 2018, **2018**, 4526396.

43 H. Zhu, J. She, M. Zhou and X. Fan, Rapid and sensitive detection of formaldehyde using portable 2-dimensional gas chromatography equipped with photoionization detectors, *Sens. Actuators, B*, 2019, **283**, 182–187.